Towards nondegenerate polarization entanglement from a waveguide down-conversion source

Meier, Kristina, Kaneda, Fumihiro, Kwiat, Paul

Kristina A. Meier, Fumihiro Kaneda, Paul G. Kwiat, "Towards nondegenerate polarization entanglement from a waveguide down-conversion source," Proc. SPIE 10659, Advanced Photon Counting Techniques XII, 106590K (14 May 2018); doi: 10.1117/12.2306532

SPIE.

Event: SPIE Commercial + Scientific Sensing and Imaging, 2018, Orlando, Florida, United States

Towards nondegenerate polarization entanglement from a waveguide down-conversion source

Kristina A. Meier, Fumihiro Kaneda, and Paul G. Kwiat

University of Illinois at Urbana-Champaign, 1110 W Green St, Urbana, Illinois, USA

ABSTRACT

As optical quantum information processing protocols and experiments become increasingly more complex, integrated optics provide a small and robust alternative to traditional bulk optics. Specifically, waveguide technology allows for the creation of bright single-photon sources based on the fact that photon pairs can be created at any location along the waveguide. For our goals, we are working on the characterization of a highly nondegenerate Spontaneous Parametric Down-Conversion (SPDC) waveguide source on a periodically poled KTP (PPKTP) crystal. Our current waveguide source uses type-II phase-matching to create collinear signal and idler photons at 1550 nm and 810 nm, respectively, with the promise of generating simultaneous time-bin and polarization entanglement in future iterations. Our intended source application is for use in quantum key distribution and superdense teleportation protocols between a space platform and collection telescopes on Earth.

Keywords: Waveguide, Integrated Photonics, SPDC, Polarization Entanglement, Single-Photon Source, Nonlinear Crystals, Photon Counting, PPKTP

1. INTRODUCTION

Current research into the improvement of integrated optics for optical quantum information processing provides insight into the exciting future of small and stable quantum devices. The ability to scale down the required area for and increase the overall stability of high-photon-number experiments is paramount for the advancement of quantum information processing protocols. Significant progress has been made in transforming bulk optics into their integrated versions, however there is still work to be done in the integration of single-photon sources. Waveguides on nonlinear crystals are a popular choice for creating photon pairs through spontaneous parametric downconversion (SPDC) and multiple groups have shown that degenerate or near-degenerate polarization entanglement on a waveguide is possible.[1,2] However, highly nondegenerate polarization entanglement using SPDC has yet to be demonstrated from a waveguide source and no waveguide sources have realized hyperentanglement simultaneous entanglement in more than one degree of freedom[3] - which can enable novel and enhanced quantum communication protocols.[4] Through creating the first-ever source of polarization and time-bin entanglement on a waveguide, we strive to make it feasible to build bright, compact, and stable single-photon sources for advanced quantum communication protocols. Our specific experiment includes characterization of a nondegenerate SPDC waveguide source on a periodically poled KTP (PPKTP) crystal.[5] Through type-II phase-matching, collinear 1550-nm signal and 810-nm idler photons are created with the potential to generate simultaneous time-bin and polarization entanglement in future iterations. One intended application of the source is for use in quantum key distribution and superdense teleportation protocols between the International Space Station and collection telescopes on Earth.[6]

With this initial waveguide source, we have measured coincidence counts at 4.7 kHz per mW of input pump power and a process-dependent coincidence to accidental ratio (CAR) up to 10.44. To improve these count rates and achieve polarization entanglement from this source, we have explored the modes of the waveguide, in which both our pump and idler wavelengths are multi-mode, the down-conversion spectrum, and the necessary temporal post-compensation to increase our entanglement visibility. The visibility for our source is defined as

Further author information: (Send correspondence to P.G.K.)
P.G.K.: E-mail: kwiat@illinois.edu, Telephone: 1 217 333 9116
K.A.M.: E-mail: kadunga2@illinois.edu, Telephone: 1 217 244 1608

Advanced Photon Counting Techniques XII, edited by Mark A. Itzler, Joe Campbell,
Proc. of SPIE Vol. 10659, 106590K · © 2018 SPIE · CCC code:
0277-786X/18/$18 · doi: 10.1117/12.2306532

$$V = \frac{DA + AD - AA - DD}{DA + AD + AA + DD} \tag{1}$$

where the first letter represents the polarization (Diagonal or Antidiagonal) of our 810 nm collection and the second represents the polarization of our 1550 nm collection, and each term represents measured coincidence counts; to date, we have achieved 34% visibility, a concurrence of 0.34, and a purity of 59.6%. We believe that several improvements will substantially improve the source quality. These include optimizing the temporal compensation, using narrowband filtering to remove residual spectral labeling where the two processes best overlap, and incorporating tapered waveguide inputs and pump mode-filtering to only allow coupling into the fundamental mode of the waveguide.

2. WAVEGUIDE MECHANISM AND EXPERIMENTAL SETUP

The first iteration of our waveguide source uses a 4-μm channel waveguide on a PPKTP crystal. Using SPDC, our single-photon source creates collinear pairs of photons at highly non-degenerate wavelengths of 810 nm and 1550 nm. Through phase-matching and a dual-poling scheme (Fig.1a), a quantum state of $|\psi\rangle = |H_{810}V_{1550}\rangle + |V_{810}H_{1550}\rangle$ is produced. Specifically, a poling period of 27 μm in the first half of the crystal produces the $|H_{810}V_{1550}\rangle$ term, and a poling period of 58 μm in the second half produces the $|V_{810}H_{1550}\rangle$ term.

Experimentally, we create these photon pairs by direct-focusing a 532-nm continuous-wave pump laser into the waveguide using a microscope objective (Fig.1b). This method of waveguide coupling can introduce various challenges due to the pump wavelength being multi-mode within the waveguide. In order to increase both the efficiency and repeatability of the quantum state, coupling into the fundamental mode of the waveguide is required. To help guarantee that this requirement is met, future iterations of our waveguide source will include

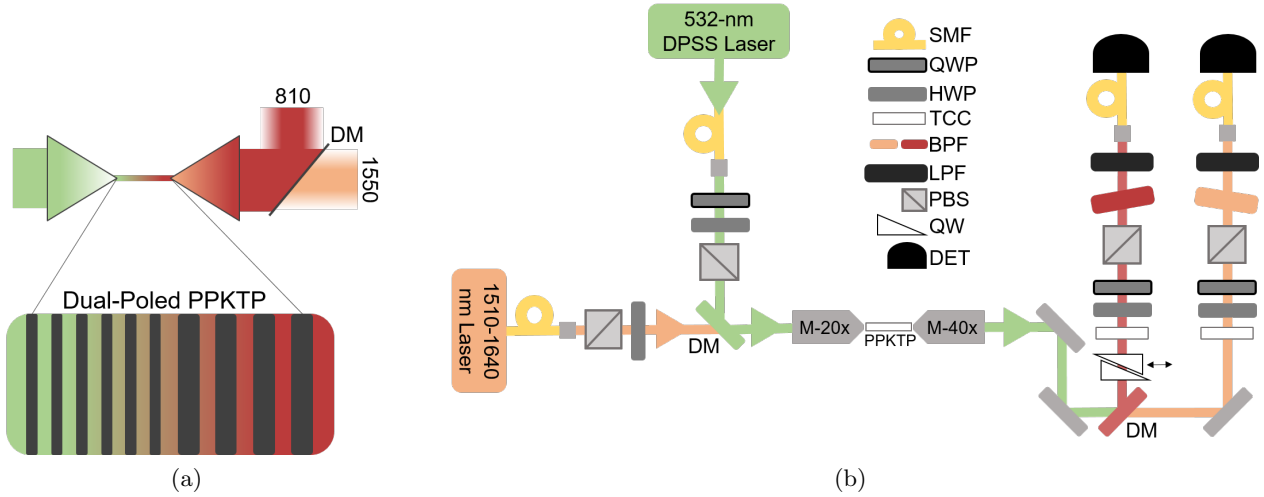

(a) (b)

Figure 1: Experimental setup for waveguide source characterization (a)A magnified view of the poling of our PPKTP crystal. The first half is poled at 27 μm and the second half at 58 μm. The free space pump and downconversion photons are direct-focused into and out of the waveguide using microscope objectives. The downconversion photons are then separated by wavelength using a dichroic mirror (DM). (b) A schematic of our characterization setup. A 532-nm pump beam is coupled into a single mode fiber (SMF) to clean up its spatial mode and then goes through a quarter waveplate (QWP), a half waveplate (HWP) and a polarizing beam splitter (PBS) to set its polarization to horizontal without losing a significant amount of power. The pump is then coupled into the waveguide using a microscope objective with 20x magnification. The resulting downconversion photons are then separated by a DM. The 810-nm (red) idler photons are sent through both a calcite temporal compensation crystal (TCC) and a pair of quartz wedges (QW) to finely adjust the necessary temporal post-compensation. The 1550-nm (orange) signal photons are sent through a calcite TCC as well. Both downconversion beams are then sent through collection optics, bandpass filters (BPF), and longpass filters (LPF) into their respective detectors (DET).

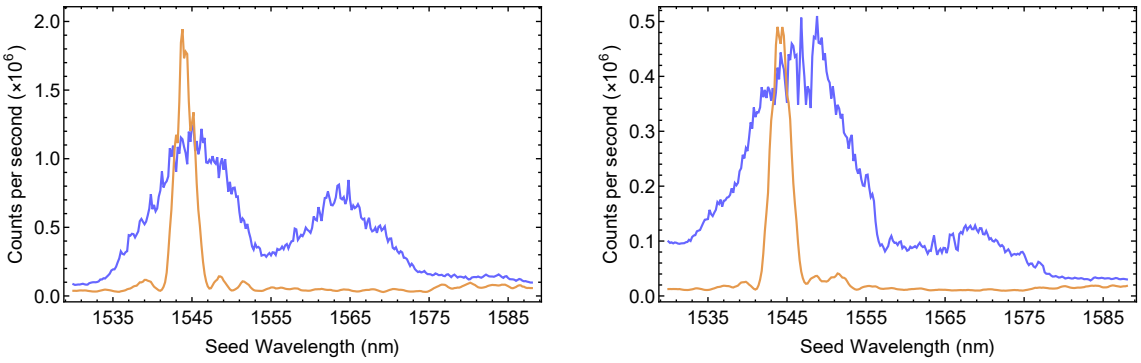

Figure 2: Stimulated downconversion measurements: the spectrums of the $H_{810}V_{1550}$ (blue) and $V_{810}H_{1550}$ (orange) are shown. (a) taken at a waveguide temperature of 40°C. (b) also taken at a waveguide temperature of 40°C a few days later. The double peak shape has diminished and the amplitudes of the two processes are equal. The comparison of the two sets of measurements suggests a strong dependency on the waveguide input coupling mode.

either input fiber-pigtailing or tapered inputs to better direct the pump into the fundamental mode of the waveguide. On exiting the waveguide, another microscope objective is used to collimate the beam and a dichroic mirror separates the downconversion photons by wavelength. The signal (1550-nm) and idler (810-nm) photons are then collected into single-mode fibers and detected on superconducting nanowire detectors ($\eta = 70 - 90\%$) and Si avalanche photodiodes ($\eta = 50\%$), respectively.

3. PHOTON-PAIR CREATION

3.1 Spectral Measurements

Before creating polarization entanglement, we first measured the central wavelengths and bandwidths of our downconversion processes. We wanted to explore not only the spectral overlap of the $H_{810}V_{1550}$ and $V_{810}H_{1550}$ processes, but also its waveguide temperature dependency. To accomplish these measurements, we coupled a tunable seed laser with a spectrum ranging from 1510 nm to 1640 nm into our waveguide source along with our pump beam. Doing so stimulates the downconversion at the chosen wavelength of the seed laser, producing high rates of single-photons at the wavelength required to meet energy conservation. With this method, we measured the resulting singles counts on the 810-nm collection side and plotted them against the wavelength of the 1550-nm seed laser as shown in Fig. 2. These spectral measurements presented three potential problems that we would need to solve. First, the downconversion spectrum was highly input-coupling-mode dependent; coupling into higher order waveguide modes, as well as accidental second harmonic generation during stimulated downconversion, can result in a varying spectrum as shown in Fig. 2. We saw that this modal effect was more prominent for the $H_{810}V_{1550}$ process, which is created in the first half of the waveguide crystal. As mentioned earlier, it is possible to near-guarantee that we couple into the fundamental mode, through fiber-pigtailing or tapering the input, which we hope to do in future iterations as we continue to work with our collaborators at AdvR, Inc. Futhermore, the bandwidths of the two processes were wildly different. For the $V_{810}H_{1550}$ process we consistently measured a nice $\text{sinc}^2(\lambda)$ function, as expected, however, for $H_{810}V_{1550}$, a broader double-peak shape is seen. To essentially erase the discrepancy in bandwidths, we filtered the outputs to help narrow the $H_{810}V_{1550}$ bandwidth. Finally, the amplitudes of the processes are different causing an imbalance between the terms of the resulting quantum state. To create a more even downconversion probability between the two processes, we can polish the end of the waveguide to slightly shorten the side of the crystal that produces the $V_{810}H_{1550}$ process.

Moreover, as we increased the waveguide temperature, we found using stimulated downconversion that the spectrum of the $H_{810}V_{1550}$ process broadens substantially faster than the $V_{810}H_{1550}$ process. Fig. 3 shows our measured idler photon counts using stimulated downconversion with a seed wavelength from 1529 nm to 1588 nm at 40°C. We should be able to further improve the source entanglement by forcing indistinguishability between

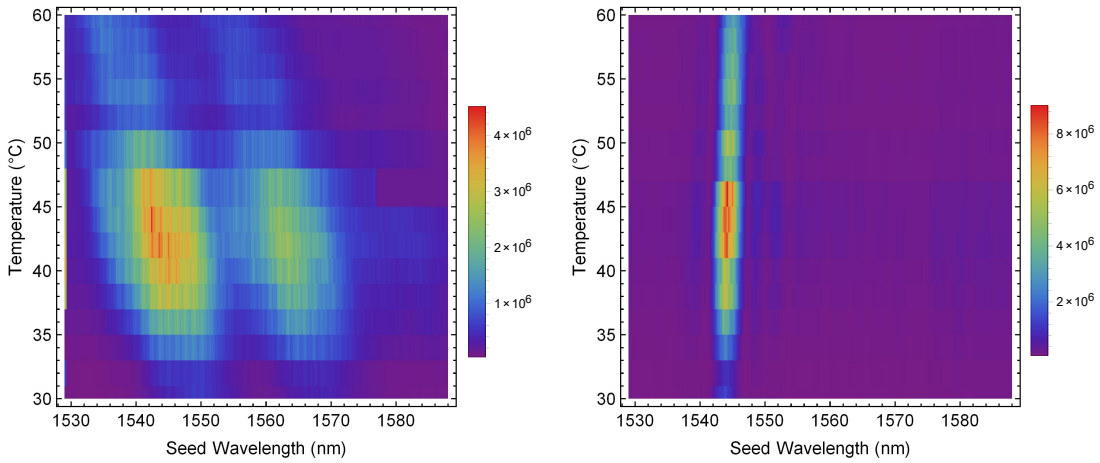

Figure 3: Temperature dependency of stimulated downconversion spectrum. The waveguide temperature was controlled using a thermoelectric cooler (TEC), from low temperatures (30°C) to high temperatures (60°C) in steps of 2°C. As noted, the process shown in (a) has a strong temperature dependence, whereas, the process shown in (b) seems near constant over temperature. The color scales, given to the right of each figure, are in units of counts per second.

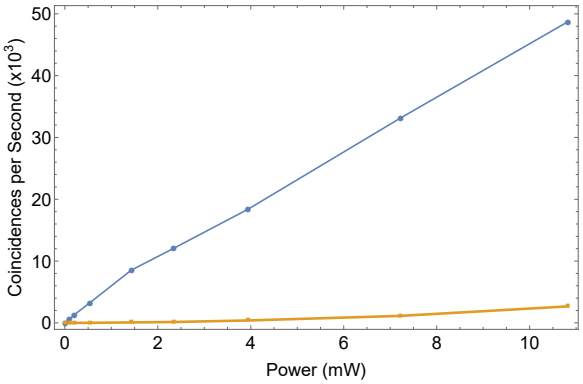

Figure 4: The measured coincidences with accidentals subtracted (blue), and accidentals (orange) per second at different pump laser powers. The power was measured immediately before the first microscope objective (M-20x in Fig. 1b), implying that less loss and therefore higher coincidences could be achieved with better mode-matching between the pump beam and the input facet of the waveguide.

the downconversion processes by implementing narrowband filters over wavelengths where there is good overlap, and by polishing down one side of the waveguide so the amplitudes of the processes are equal or coupling into a mode that gives equal amplitudes as in Fig. 2b.

3.2 Brightness and Efficiency Measurements

We have yet to make precise measurements of the brightness and efficiency of our photon-pair source; however, we have found that the brightness and CAR of the current iteration is sufficient for measuring the capability of our source to create polarization-entangled pairs. For the current setup, we have achieved a CAR of 10.44 for $H_{810}V_{1550}$ and 3.26 for $V_{810}H_{1550}$. Fig. 4 shows the coincidences per second per input power (measured immediately before the first microscope objective, M-20x). Another metric we use to estimate the downconversion state is the coincidence cross correlation (CCC) for each polarization combination. For a given polarization combination, the CCC measures the coincidence counts for different delays between the 1550 collection and the 810 collection, allowing us to find the relative time difference between when the signal and idler photons arrive at their respective detectors. Fig. 5 shows the CCC measurements for $H_{810}V_{1550}$, $V_{810}H_{1550}$, $V_{810}V_{1550}$, and $H_{810}H_{1550}$. Figures 5a and 5b show nice peaks that are well above the background level as expected for the

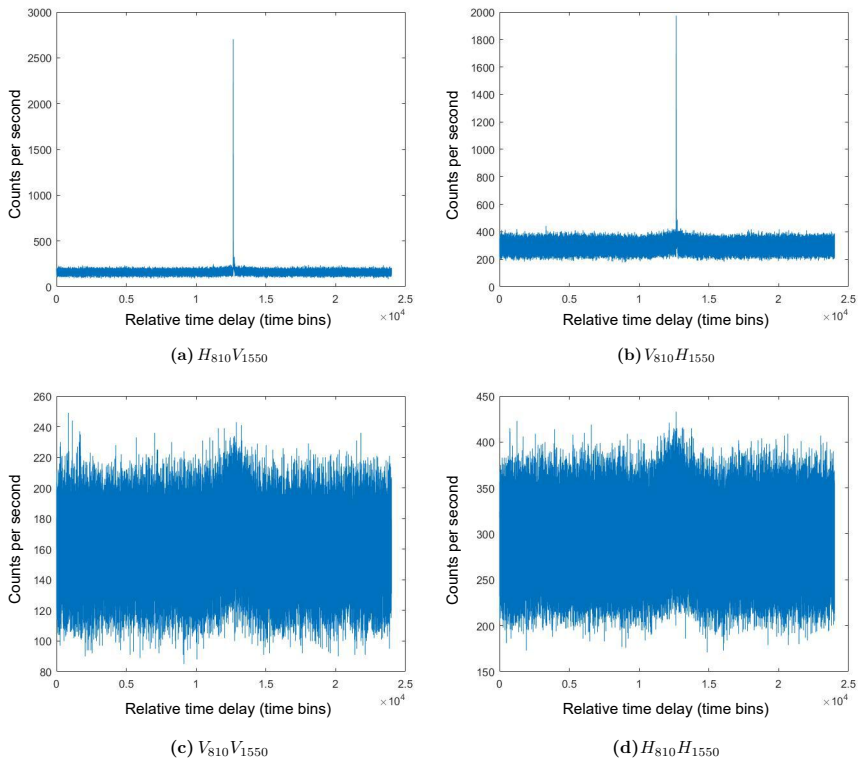

(a) $H_{810}V_{1550}$ (b) $V_{810}H_{1550}$

(c) $V_{810}V_{1550}$ (d) $H_{810}H_{1550}$

Figure 5: Coincidence cross correlation measurements for four different polarization combinations. (a) and (b) show coincidence peaks for the desired processes well above the background noise, shown in (c) and (d). These measurements show that our waveguide source is producing the expected processes attributing only random noise created by background counts and possible fluorescence to the counts in (c) and (d). The width of our time bins is 156 ps.

desired quantum state, while figures 5c and 5d both show that the coincidence counts for those processes are at level of the background counts.

4. POLARIZATION ENTANGLEMENT

Creating polarization-entangled photon pairs with high visibility requires there to be no information about where the photons were created. Given the dual-poling scheme implemented in our waveguide source, photons created in the first half of the PPKTP crystal are temporally separated from those created in the second half. Furthermore, the temporal walk-off within the crystal, meaning the two polarizations, horizontal and vertical, travel at different speeds through the birefringent material, causes the downconversion photons to exit the crystal at different times. In addition to the temporal walkoff within the crystal, it is possible that there is some phase between the terms of the desired quantum state as shown in Eq. 2:

$$\mid \psi\rangle = \alpha \mid H_{810}V_{1550}\rangle + e^{i\phi}\beta \mid V_{810}H_{1550}\rangle \tag{2}$$

where ϕ is some arbitrary phase and α and β correspond to the relative amplitudes of the two processes. Although this phase does not affect the amount of entanglement, it does hinder our ability to create the desired state. Finally, any differences in the amplitudes or bandwidths of these two processes (as shown in 3.1) can degrade the overall visibility of the entangled state.

These problems are not unique to waveguide sources; any bulk SPDC source where the two processes are created in two separate locations, as in a double-crystal SPDC scheme,[7] will have to account for walk-off within the crystal unless the SPDC coherence length is sufficiently long. To compensate for this, a birefringent crystal is placed in the setup to effectively temporally overlap the downconversion photons. Frequently, one crystal can

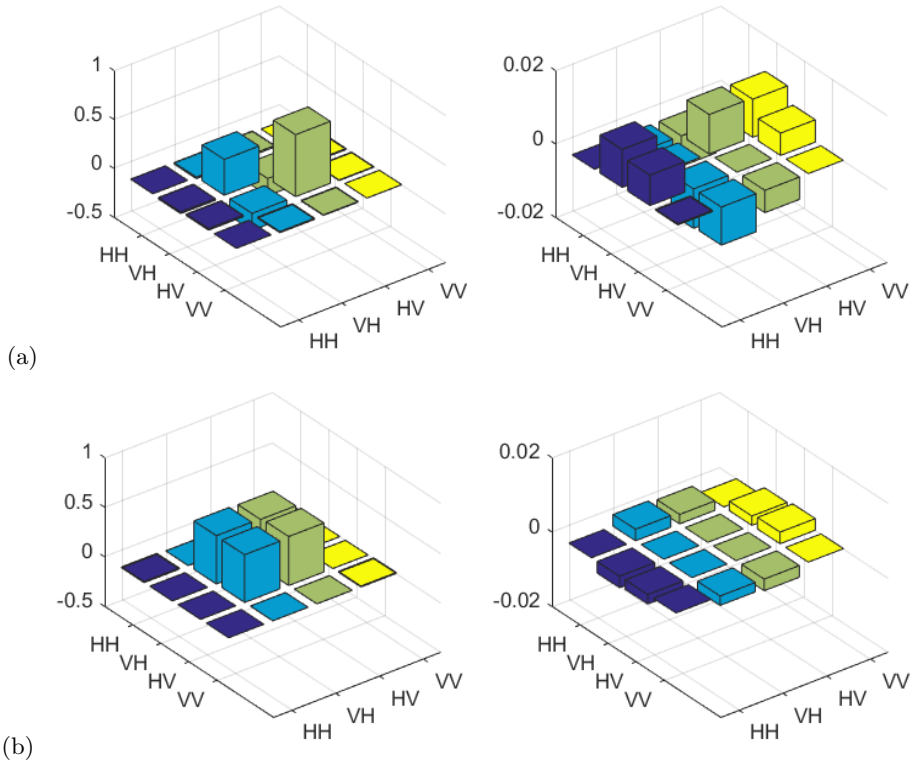

Figure 6: (a) Measured density matrix giving a concurrence of 0.34 and purity of 59.6%. (b) Theoretical density matrix for the state, $|\psi\rangle = \frac{1}{\sqrt{2}}(|H_{810}V_{1550}\rangle + |V_{810}H_{1550}\rangle)$. The left images are the real parts of their respective density matrix and the right images are the imaginary parts.

be used before the source to pre-compensate for the walk-off. However, since we are pumping with horizontally-polarized light, pre-compensation is not possible. For our source, individual compensation in both collection sides is required to temporally match the H_{810} and V_{810} photons and the H_{1550} and V_{1550} photons. Specifically, as shown in Fig.1b, we use a set of calcite crystals for coarse compensation and a pair of quartz wedges for fine adjustments. Quartz is roughly 18 times less birefringent than calcite for both downconversion wavelengths, making it an appropriate choice for fine tuning the temporal compensation. To account for the other visibility-reducing factors in our experiment, carefully tuned bandpass filters, more careful waveguide design in our second iteration, and phase adjustment using liquid crystals can be pursued. Currently, by tilting our bandpass filters to tune the transmission spectrum and adding a not necessarily optimal amount of temporal compensation, we have achieved a visibility of 34%. Future measurements will include a continuation of using the quartz wedges to better tune the temporal compensation, performing various experiments with the liquid crystals to find the optimal phase correction, and better overall mode-matching between the pump laser and the waveguide.

Finally, to reconstruct the density matrix of the quantum state produced by this setup, we perform a two-qubit state tomography on the measured downconversion photons, as shown in Fig. 6. To do so, various polarization optics in both collection sides are used to measure the 36 polarization combinations needed to calculate the density matrix.[8] We can then compare our measured density matrix to the theoretical one to better guide us in our source optimization.

5. CONCLUSION

Movement towards integrated single-photon sources promises a bright future for quantum information protocols requiring large amounts of bulk optics. With future iterations of our source, we hope to create a bright, robust,

and fully-integrated source that creates highly non-degenerate polarization and time-bin entangled single-photon pairs.

ACKNOWLEDGMENTS

This research was funded by NASA Grant No. NNX16AM26G and conducted with Government support under and awarded by DoD, Air Force Office of Scientific Research, National Defense Science and Engineering Graduate (NDSEG) Fellowship, 32 CFR 168a. A special thank you to AdvR Inc. in Bozeman, MT for designing the current and future iterations of our waveguide source and for their continued correspondence.

REFERENCES

[1] Herrmann, H., Yang, X., Thomas, A., Poppe, A., Sohler, W., and Silberhorn, C., "Post-selection free, integrated optical source of non-degenerate, polarization entangled photon pairs," *Opt. Express* **21**, 27981–27991 (2013).

[2] [*Generating entangled photons on monolithic chips*], **10547** (2018).

[3] Barreiro, J. T., Langford, N. K., Peters, N. A., and Kwiat, P. G., "Generation of hyperentangled photon pairs," *Phys. Rev. Lett.* **95**, 260501 (Dec 2005).

[4] Barreiro, J. T., Wei, T.-C., and Kwiat, P. G., "Beating the channel capacity limit for linear photonic superdense coding," *Nature Physics* **4** (Aug 2008).

[5] Advr-Inc. Bozeman, MT.

[6] [*Proc. SPIE 9739, Free-Space Laser Communication and Atmospheric Propagation XXVIII (DISC 2016)*], *LNCS* **9739**, SPIE (2016).

[7] Kwiat, P. G., Mattle, K., Weinfurter, H., Zeilinger, A., Sergienko, A. V., and Shih, Y., "New high-intensity source of polarization-entangled photon pairs," *Phys. Rev. Lett.* **75**, 4337–4341 (Dec 1995).

[8] James, D. F. V., Kwiat, P. G., Munro, W. J., and White, A. G., "Measurement of qubits," *Phys. Rev. A* **64**, 052312 (Oct 2001).